Methane−Methanol Conversion by MnO^+, FeO^+, and CoO^+: A Theoretical Study of Catalytic Selectivity

Kazunari Yoshizawa,*,† Yoshihito Shiota,† and Tokio Yamabe†,‡

Contribution from the Department of Molecular Engineering, Kyoto University, Sakyo-ku, Kyoto, 606-01 Japan, and Institute for Fundamental Chemistry, 34-4 Takano-Nishihiraki-cho, Sakyo-ku, Kyoto, 606 Japan

Received May 27, 1997

Abstract: The entire reaction pathway for the gas-phase methane−methanol conversion by late transition-metal-oxide ions, MnO^+, FeO^+, and CoO^+, is studied using an ab initio hybrid (Hartree−Fock/density-functional) method. For these oxo complexes, the methane−methanol conversion is proposed to proceed via two transition states (TSs) in such a way $MO^+ + CH_4 \rightarrow OM^+(CH_4) \rightarrow$ [TS1] $\rightarrow HO-M^+-CH_3 \rightarrow$ [TS2] $\rightarrow M^+(CH_3OH) \rightarrow M^+ + CH_3OH$, where M is Mn, Fe, and Co. A crossing between high-spin and low-spin potential energy surfaces occurs both at the entrance channel and at the exit channel for FeO^+ and CoO^+, but it occurs only once near TS2 for MnO^+. The activation energy from $OMn^+(CH_4)$ to $HO-Mn^+-CH_3$ via TS1 is calculated to be 9.4 kcal/mol, being much smaller than 22.1 and 30.9 kcal/mol for FeO^+ and CoO^+, respectively. This agrees with the experimentally reported efficiencies for the reactions. The excellent agreement between theory and experiment indicates that $HO-M^+-CH_3$ plays a central role as an intermediate in the reaction between MO^+ and methane and that the reaction efficiency is most likely to be determined by the activation energy from $OM^+(CH_4)$ to $HO-M^+-CH_3$ via TS1. We discuss in terms of qualitative orbital interactions why MnO^+ (d^4 oxo complex) is most effective for methane C−H bond activation. The activation energy from $HO-M^+-CH_3$ to $M^+(CH_3OH)$ via TS2 is computed to be 24.6, 28.6, and 35.9 kcal/mol for CoO^+, FeO^+, and MnO^+, respectively. This result explains an experimental result that the methanol-branching ratio in the reaction between MO^+ and methane is 100% in CoO^+, 41% in FeO^+, and < 1% in MnO^+. We demonstrate that both the barrier heights of TS1 and TS2 would determine general catalytic selectivity for the methane−methanol conversion by the MO^+ complexes.

Introduction

The activation of methane[1−9] has attracted increased attention in recent years because of its scientific and industrial importance. In particular, methanol converted from methane is likely to be of great interest as an important energy source in the 21st century. An industrial process for the production of methanol from natural gas that mainly consists of methane involves two-step reactions associated with the formation of synthesis gas, i.e., carbon monoxide.[6] The so-called Fischer−Tropsch reaction converts carbon monoxide into a mixture of long-chain alkanes and alcohols. The conversion of methane to methanol is also known to occur very efficiently when catalyzed enzymatically, e.g., by methane monooxygenase (MMO).[10] We have been interested in the conversion of methane to methanol catalyzed by MMO from a theoretical viewpoint.[11]

The gas-phase C−H and C−C bond activations of small hydrocarbons (by various transition-metal-oxide ions and bare metal cations) have been experimentally and theoretically investigated in Schwarz's[12] and Armentrout's[13] laboratories. Detailed analyses of various gas-phase reactions of methane, higher alkanes, alkenes, benzene, and other [C, H, O] com-

† Kyoto University.

‡ Institute for Fundamental Chemistry.

(1) Shilov, A. E. *The Activation of Saturated Hydrocarbons by Transition Metal Complexes*; Reidel: Dortrecht, 1984.

(2) (a) Bergman, R. G. *Science* **1984**, *223*. 902. (b) Arndtsen, B. A.; Bergman, R. G.; Mobley, T. A.; Peterson, T. H. *Acc. Chem. Res* **1995**, *28*, 154.

(3) Hill, C. L., Ed. *Activation and Functionalization of Alkanes*; Wiley: New York, 1989.

(4) Davies, J. A.; Watson, P. L.; Liebman, J. F.; Greenberg, A. *Selective Hydrocarbon Activation*; VCH: New York, 1990.

(5) (a) Crabtree, R. H. *The Organometallic Chemistry of The Transition Metals*; Wiley: New York, 1994. (b) Crabtree, R. H. *Chem. Rev. (Washington, D.C.)* **1985**, *85*, 245. (c) Crabtree, R. H. *Chem. Rev. (Washington, D.C.)* **1995**, *95*, 987.

(6) Gesser, H. D.; Hunter, N. R.; Prakash, C. B. *Chem. Rev.* **1985**, *85*, 237.

(7) Lunsford, J. H. *Angew. Chem., Int. Ed. Engl.* **1995**, *34*, 970.

(8) Schneider, J. J. *Angew. Chem., Int. Ed. Engl.* **1996**, *35*, 1068.

(9) Hall, C.; Perutz, R. N. *Chem. Rev. (Washington, D.C.)* **1996**, *96*, 3125.

(10) Recent reviews on methane monooxygenase and other non-heme diiron enzymes: (a) Wallar, B. J.; Lipscomb, J. D. *Chem. Rev. (Washington, D.C.)* **1996**, *96*, 2625. (b) Que, L. Jr.; Dong, Y. *Acc. Chem. Res* **1996**, *29*, 190. (c) Feig, A. L.; Lippard, S. J. *Chem. Rev. (Washington, D.C.)* **1994**, *94*, 759. (d) Stenkamp, R. E. *Chem. Rev.* **1994**, *94*, 715. (e) Lipscomb, J. D. *Annu. Rev. Microbiol.* **1994**, *48*, 371. (f) Lippard, S. J. *Angew. Chem., Int. Ed. Engl.* **1988**, *27*, 344.

(11) (a) Yoshizawa, K.; Hoffmann, R. *Inorg. Chem.* **1996**, *35*, 2409. (b) Yoshizawa, K.; Yamabe, T.; Hoffmann, R. *New J. Chem.* **1997**, *21*, 151. (c) Yoshizawa, K.; Yokomichi, Y.; Shiota, Y.; Ohta, T.; Yamabe, T. *Chem. Lett.* **1997**, 587. (d) Yoshizawa, K.; Ohta, T.; Shiota, Y.; Yamabe, T. *Chem. Lett.* **1997**, 1213. (e) Yoshizawa, K. *J. Biol. Inorg. Chem.* **1998**, in press.

(12) (a) Schröder, D.; Schwarz, H. *Angew. Chem., Int. Ed. Engl.* **1990**, *29*, 1433. (b) Schwarz, H. *Angew. Chem., Int. Ed. Engl.* **1991**, *30*, 820. (c) Schröder, D.; Fiedler, A.; Hrušák, J.; Schwarz, H. *J. Am. Chem. Soc.* **1992**, *114*, 1215. (d) Fiedler, A.; Hrušák, J.; Koch, W.; Schwarz, H. *Chem. Phys. Lett.* **1993**, *211*, 242. (e) Fiedler, A.; Schröder, D.; Shaik, S.; Schwarz, H. *J. Am. Chem. Soc.* **1994**, *116*, 10734. (f) Schröder, D.; Schwarz, H. *Angew. Chem., Int. Ed. Engl.* **1995**, *34*, 1973. (g) Wesendrup, R.; Schalley, C. A.; Schröder, D.; Schwarz, H. *Chem. Eur. J.* **1995**, *1*, 608. (h) Shaik, S.; Danovich, D.; Fiedler, A.; Schröder, D.; Schwarz, H. *Helv. Chim. Acta* **1995**, *78*, 1393. (i) Ryan, M. F.; Fiedler, A.; Schröder, D.; Schwarz, H. *J. Am. Chem. Soc.* **1995**, *117*, 2033. (j) Holthausen, M. C.; Fiedler, A.; H. Schwarz, W. Koch, *J. Phys. Chem.* **1996**, *100*, 6236. (k) Fiedler, A.; Schröder, D.; Schwarz, H.; Tjelta, B. L.; Armentrout, P. B. *J. Am. Chem. Soc.* **1996**, *118*, 5047.

S0002-7863(97)01723-X CCC: $15.00 © 1998 American Chemical Society
Published on Web 01/06/1998

Scheme 1

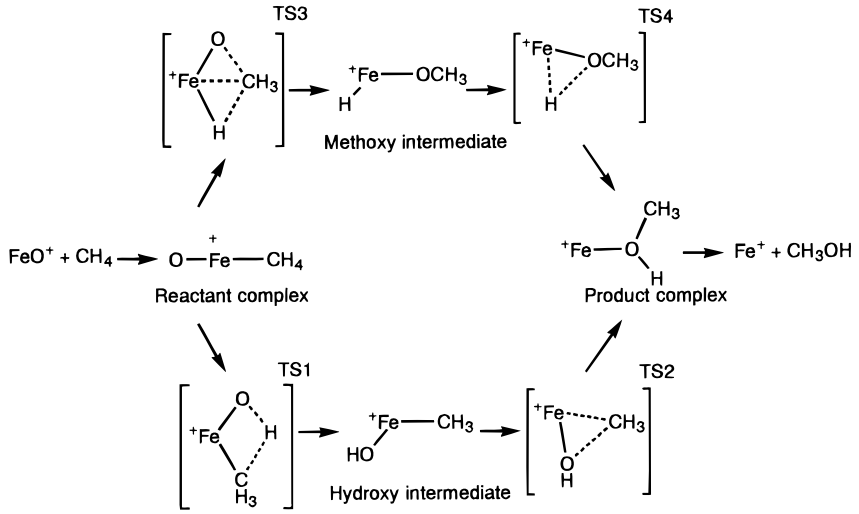

pounds with transition-metal oxides have been carried out. Among these important gas-phase reactions, the methane−methanol conversion by metal-oxide ions is of particular interest since this process may be viewed as the simplest model for alkane hydroxylation. On the basis of experimentally determined isotope effects, Schröder and Schwarz[12a,b] have suggested that a reaction species, $HO-Fe^+-CH_3$, is a central intermediate in the reaction between FeO^+ and CH_4. Armentrout et al.[13j] have investigated the mechanism and energetics involved in the gas-phase methane−methanol conversion by CoO^+ and its reverse reaction. An insertion intermediate, $HO-Co^+-CH_3$, has been also suggested to play an important role in this gas-phase reaction. However, the efficiency of the reaction of CoO^+ with methane is low as compared with that of FeO^+. Recently related ion-molecular complexes of $M^+(CH_4)$ and C−H bond activation of methane have been reported by many authors.[14]

On methane and C−H bond activation, there has been a large amount of theoretical work by Saillard and Hoffmann,[15] Goddard et al.,[16] Siegbahn and Blomberg and their collaborators,[17] Ziegler et al.,[18] Morokuma et al.,[19] Sakaki and Ieki,[20] and Cundari.[21] In a recent paper,[22] we have proposed two kinds of entire reaction pathways for the gas-phase methane−methanol conversion by FeO^+ on the basis of detailed IRC (intrinsic reaction coordinate)[23] analyses. The reaction pathways proposed in the paper proceed via two kinds of important reaction intermediates, $HO-Fe^+-CH_3$ and $H-Fe^+-OCH_3$, as shown in Scheme 1. Our ab initio (Hartree−Fock/density-functional) calculations showed that the reaction pathway via the hydroxy intermediate ($HO-Fe^+-CH_3$) is energetically more favorable than the other one via the methoxy intermediate ($H-Fe^+-OCH_3$). This result is consistent with the prediction by Schwarz and collaborators that $HO-Fe^+-CH_3$ plays a central role in the gas-phase reaction between FeO^+ and methane.

The Berlin group[12f] has systematically examined the efficiency and product branching ratio for the gas-phase reactions of various transition-metal-oxide ions with methane. Although early transition-metal-oxide ions, ScO^+, TiO^+, VO^+, and CrO^+, do not react with methane, it is well established that oxide ions of late transition metals, MnO^+, FeO^+, CoO^+, and NiO^+, react with methane. Table 1 lists only a part of experimental results reported in ref 12f. As seen in the table, MnO^+ has a high reaction efficiency, but unfortunately the methanol-branching

(13) (a) Aristov, N.; Armentrout, P. B. *J. Phys. Chem.* **1987**, *91*, 6178. (b) Shultz, R. H.; Elkind, J. L.; Armentrout, P. B. *J. Am. Chem. Soc.* **1988**, *110*, 411. (c) Sunderlin, L. S.; Armentrout, P. B. *J. Phys. Chem.* **1988**, *92*, 1209. (d) Geoorgiadis, R.; Armentrout, P. B. *J. Phys. Chem.* **1988**, *92*, 7060. (e) Armentrout, P. B.; Beauchamp, J. L. *Acc. Chem. Res* **1989**, *22*, 315. (f) van Koppen, P. A. M.; Brodbelt-Lustig, J.; Bowers, M. T.; Dearden, D. V.; Beauchamp, J. L.; Fisher, E. R.; Armentrout, P. B. *J. Am. Chem. Soc.* **1990**, *112*, 5663. (g) Armentrout, P. B. *Science* **1991**, *251*, 175. (h) van Koppen, P. A. M.; Brodbelt-Lustig, J.; Bowers, M. T.; Dearden, D. V.; Beauchamp, J. L.; Fisher, E. R.; Armentrout, P. B. *J. Am. Chem. Soc.* **1991**, *113*, 2359. (i) Clemmer, D. E.; Aristov, N.; Armentrout, P. B. *J. Phys. Chem.* **1993**, *97*, 544. (j) Chen, Y.-M.; Clemmer, D. E.; Armentrout, P. B. *J. Am. Chem. Soc.* **1994**, *116*, 7815. (k) Clemmer, D. E.; Chen, Y.-M.; Kahn, F. A.; Armentrout, P. B. *J. Phys. Chem.* **1994**, *98*, 6522.

(14) (a) Trevor, D. J.; Cox, D. M.; Kaldor, A. *J. Am. Chem. Soc.* **1990**, *112*, 3742. (b) Irikura, K. K.; Beauchamp, J. L. *J. Phys. Chem.* **1991**, *95*, 8344. (c) Ranasinghe, Y. A.; MacMahon, T. J.; Freiser, B. S. *J. Phys. Chem.* **1991**, *95*, 7721. (d) Van Zee, R. J.; Li, S.; Weltner, W., Jr. *J. Am. Chem. Soc.* **1993**, *115*, 2976. (e) Carrol, J. J.; Weisshaar, J. C. *J. Am. Chem. Soc.* **1993**, *115*, 800. (f) Burger, P.; Bergman, R. G. *J. Am. Chem. Soc.* **1993**, *115*, 10462. (g) Schaller, C. P.; Bonanno, J. B.; Wolczanski, P. T. *J. Am. Chem. Soc.* **1994**, *116*, 4133. (h) Zhang, X.-X.; Wayland, B. B. *J. Am. Chem. Soc.* **1994**, *116*, 7897. (i) Billups, W. E.; Chang, S.-C.; Hauge, R. H.; Margrave, J. L. *J. Am. Chem. Soc.* **1995**, *117*, 1387. (j) van Koppen, P. A. M.; Kemper, P. R.; Bushnell, J. E.; Bowers, M. T. *J. Am. Chem. Soc.* **1995**, *117*, 2098. (k) Campbell, M. L. *J. Am. Chem. Soc.* **1997**, *119*, 5984.

(15) (a) Saillard, J.-Y.; Hoffmann, R. *J. Am. Chem. Soc.* **1984**, *106*, 2006. (b) Hoffmann, R. *Rev. Mod. Phys.* **1988**, *60*, 601.

(16) (a) Low, J. J.; Goddard, W. A. III *J. Am. Chem. Soc.* **1984**, *106*, 8321. (b) Low, J. J.; Goddard, W. A. III *J. Am. Chem. Soc.* **1986**, *108*, 6115. (c) Perry, J. K.; Ohanessian, G.; W. A. Goddard, W. A. III *J. Phys. Chem.* **1993**, *97*, 5238.

(17) (a) Blomberg, M. R. A.; Brandemark, U.; Siegbahn, P. E. M. *J. Am. Chem. Soc.* **1983**, *105*, 5557. (b) Blomberg, M. R. A.; Siegbahn, P. E. M.; Nagashima, U.; Wennerberg, J. *J. Am. Chem. Soc.* **1991**, *113*, 424. (c) Blomberg, M. R. A.; Siegbahn, P. E. M.; Svensson, M. *J. Am. Chem. Soc.* **1992**, *114*, 6095. (d) Siegbahn, P. E. M.; Blomberg, M. R. A. *Organometallics* **1994**, *13*, 354. (e) Siegbahn, P. E. M. *Organometallics* **1994**, *13*, 2833. (f) Siegbahn, P. E. M. *J. Am. Chem. Soc.* **1996**, *118*, 1487. (g) Siegbahn, P. E. M.; Crabtree, R. H. *J. Am. Chem. Soc.* **1996**, *118*, 4442.

(18) (a) Ziegler, T.; Tschinke, V.; Becke, A. D. *J. Am. Chem. Soc.* **1987**, *109*, 1351. (b) Ziegler, T.; Tschinke, V.; Fan, L.; Becke, A. D. *J. Am. Chem. Soc.* **1989**, *111*, 9177. (c) Ziegler, T.; Folga, E.; Berces, A. *J. Am. Chem. Soc.* **1993**, *115*, 636.

(19) (a) Koga, N.; Morokuma, K. *J. Phys. Chem.* **1990**, *94*, 5454. (b) Koga, N.; Morokuma, K. *J. Am. Chem. Soc.* **1993**, *115*, 6883. (c) Musaev, D. G.; Koga, N.; Morokuma, K. *J. Phys. Chem.* **1993**, *97*, 4064. (d) Musaev, D. G.; Morokuma, K.; Koga, N.; Ngyen, K.; Gordon, M. S.; Cundari, T. R. *J. Phys. Chem.* **1993**, *97*, 11435. (e) Musaev, D. G.; Morokuma, K. *J. Chem. Phys.* **1994**, *101*, 10697. (f) Musaev, D. G.; Morokuma, K. *J. Phys. Chem.* **1996**, *100*, 11600.

(20) (a) Sakaki, S.; Ieki, M. *J. Am. Chem. Soc.* **1991**, *113*, 5063. (b) Sakaki, S.; Ieki, M. *J. Am. Chem. Soc.* **1993**, *115*, 2373.

(21) (a) Cundari, T. R. *J. Am. Chem. Soc.* **1992**, *114*, 10557. (b) Cundari, T. R.; Gordon, M. S. *J. Am. Chem. Soc.* **1993**, *115*, 4210. (c) Cundari, T. R. *J. Am. Chem. Soc.* **1994**, *116*, 340.

(22) Yoshizawa, K.; Shiota, Y.; Yamabe. T. *Chem. Eur. J.* **1997**, *3*, 1160.

(23) (a) Fukui, K. *J. Phys. Chem.* **1970**, *74*, 4161. (b) Fukui, K. *Acc. Chem. Res* **1981**, *14*, 363.

Table 1. Reaction Efficiencies ϕ (%) and Product Branching Ratios (%) for the Reactions of Methane with Late Transition-Metal-Oxide Ions[a]

MO^+	ϕ	$MOH^+ + CH_3$	$MCH_2^+ + H_2O$	$M^+ + CH_3OH$
MnO^+	40	100		<1
FeO^+	20	57	2	41
CoO^+	0.5			100

[a] Data from ref 12f.

ratio is very low. On the other hand, the reaction efficiency of CoO^+ is very low, but its methanol-branching ratio is 100%. For the reaction between FeO^+ and methane there are two main competitive reaction pathways that lead to $FeOH^+ + {}^\bullet CH_3$ and $Fe^+ + CH_3OH$. Formation of water is a minor branch in the reaction between the MO^+ ions and methane.

In this theoretical work we would like to elucidate the selectivity of the reactions by these MO^+ complexes. If the reaction mechanism in Scheme 1 is true, one expects from Table 1 that the activation energy from $OMn^+(CH_4)$ to $HO-Mn^+-CH_3$ via TS1 should be small, but that from $HO-Mn^+-CH_3$ to $Mn^+(CH_3OH)$ via TS2 should be large. In contrast, the activation energy from $CoO^+(CH_4)$ to $HO-Co^+-CH_3$ should be large, but that from $HO-Co^+-CH_3$ to $Co^+(CH_3OH)$ should be small. To understand the reason the reaction efficiencies and the product branching ratios are different in different metal-oxide ions, we have theoretically investigated the reactivities of MnO^+, FeO^+, and CoO^+ with methane.

The formal charges of the metal active centers of MnO^+, FeO^+, and CoO^+ are +3, and therefore they are supposed to be d^4, d^5, and d^6 electronic systems, respectively. It is likely to be of interest to broad area of chemistry to compare the reactivities of these late transition-metal-oxide ions. A purpose in this paper is to explain how the reaction efficiency changes as a function of the number of d electrons in transition-metal complexes.

Method of Calculation

The two kinds of reaction pathways (from methane to methanol) indicated in Scheme 1 were computed using the Gaussian 94 ab initio program package.[24] We compared the reactivities of MnO^+, CoO^+, and FeO^+ with methane. We optimized local minima (on a potential energy hypersurface) corresponding to the reactant complexes, $OM^+(CH_4)$, reaction intermediates, $HO-M^+-CH_3$ and $H-M^+-OCH_3$, and product complexes, $M^+(CH_3OH)$, using the hybrid (Hartree−Fock/density functional theory) B3LYP method. It consists of the Slater exchange, the Hartree−Fock exchange, the exchange functional of Becke,[25] the correlation functional of Lee, Yang, and Parr (LYP),[26] and the correlation functional of Vosco, Wilk, and Nusair.[27] The contribution of each energy to the B3LYP energy expression was fitted[25] empirically on a reference set of molecules. For Mn, Fe, and Co atoms we used the (14s9p5d) primitive set of Wachters[28] supplemented with one polarization f-function (α = 0.96 for Mn, 1.05 for Fe, and 1.17 for Co)[29] resulting in a (611111111|51111|311|1) [9s5p3d1f] contraction, and for H, C, and O atoms we used the 6-311G** basis set of Pople and co-workers.[30] These are referred to below as 6-311G** following the basis set code of Gaussian 94. Transition-state (TS) structures were also optimized at the same level of theory. Glukhovtesev et al.[31] recently reported excellent performance of the B3LYP method (combined with effective core potentials) for iron-containing complexes. Vibrational frequencies were systematically computed in order to ensure that on a potential energy surface all optimized geometries correspond to a local minimum that has all real frequencies or a saddle point that has only one imaginary frequency. Zero-point energy corrections were taken into account in calculating the total energies of the reactant complexes, intermediates, product complexes, and TSs. Sextet and quartet spin states were considered for FeO^+ cases; quintet and triplet states for CoO^+ cases; septet and quintet states for MnO^+ cases. The spin-unrestricted method was applied to such open-shell systems. Computed $\langle S^2 \rangle$ values confirmed that spin contamination included in calculations was very small (within 0.4% after annihilation of spin contamination). To estimate the binding energy for the formation of the reactant complex and the dissociation energy toward the products, i.e., methanol and the M^+ ion, we calculated the electronic structures of the MO^+ complexes and the M^+ ions within the framework of the B3LYP method.

Scheme 2

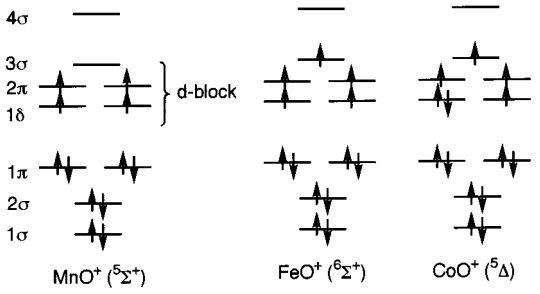

General Electronic Features of Transition-Metal Oxide Ions

Before describing the conversion of methane to methanol by MnO^+, FeO^+, and CoO^+, we refer to the general electronic features of transition-metal-oxide ions. Carter and Goddard[32] predicted the general bonding characters of first-row MO^+ complexes from generalized valence bond calculations. The reactivity of MO^+ complexes has been proposed to be understood by considering how the d-block orbitals are occupied−early transition metals form strong, unreactive triple bonds and late transition metals form weak, reactive biradical double bonds. Moreover, Schwarz's group[12d,e,h] calculated (using a density functional method) the electronic structures of late transition-metal-oxide ions, FeO^+-CuO^+, and examined the reactivity of FeO^+ with dihydrogen.

Scheme 2 shows the molecular orbital diagrams for the ground states of MnO^+ ($^5\Sigma^+$), FeO^+ ($^6\Sigma^+$), and CoO^+ ($^5\Delta$). For MnO^+, the lowest-lying $^5\Sigma^+$ state has been calculated to be slightly below the $^5\Pi$ ($1\sigma^2 2\sigma^2 1\pi^4 1\delta^3 2\pi^1 3\sigma^1$) state, and the $^7\Pi$

(24) Frisch, M. J.; Trucks, G. W.; Schlegel, H. B.; Gill, P. M. W.; Johnson, B. G.; Robb, M. A.; Cheeseman, J. R.; Keith, T. A.; Petersson, G. A.; Montgomery, J. A.; Raghavachari, K.; Al-Laham, M. A.; Zakrzewski, V. G.; Ortiz, J. V.; Foresman, J. B.; Cioslowski, J.; Stefanov, B. B.; Nanayakkara, A.; Challacombe, M.; Peng, C. Y.; Ayala, P. Y.; Chen, W.; Wong, M. W.; Andres, J. L.; Replogle, E. S.; Gomperts, R.; Martin, R. L.; Fox, D. J.; Binkley, J. S.; Defrees, D. J.; Baker, J.; Stewart, J. J. P.; Head-Gordon, M.; Gonzalez, C.; Pople, J. A. *Gaussian 94*; Gaussian Inc.: Pittsburgh, PA, 1995.

(25) (a) Becke, A. D. *Phys. Rev.* **1988**, *A38*, 3098. (b) Becke, A. D. *J. Chem. Phys.* **1993**, *98*, 5648.

(26) Lee, C.; Yang, W.; Parr, R. G. *Phys. Rev.* **1988**, *B37*, 785.

(27) Vosco, S. H.; Wilk, L.; Nusair, M. *Can. J. Phys.* **1980**, *58*, 1200.

(28) Wachters, A. J. H. *J. Chem. Phys.* **1970**, *52*, 1033.

(29) Raghavachari, K.; Trucks, G. W. *J. Chem. Phys.* **1989**, *91*, 1062.

(30) Krishnan, R.; Binkley, J. S.; Seegar, R.; Pople, J. A. *J. Chem. Phys.* **1980**, *72*, 650.

(31) Glukhovtsev, M. N.; Bach, R. D.; Nagel, C. J. *J. Phys. Chem. A* **1997**, *101*, 316.

(32) Carter, E. A.; Goddard, W. A. III *J. Phys. Chem.* **1988**, *92*, 2109.

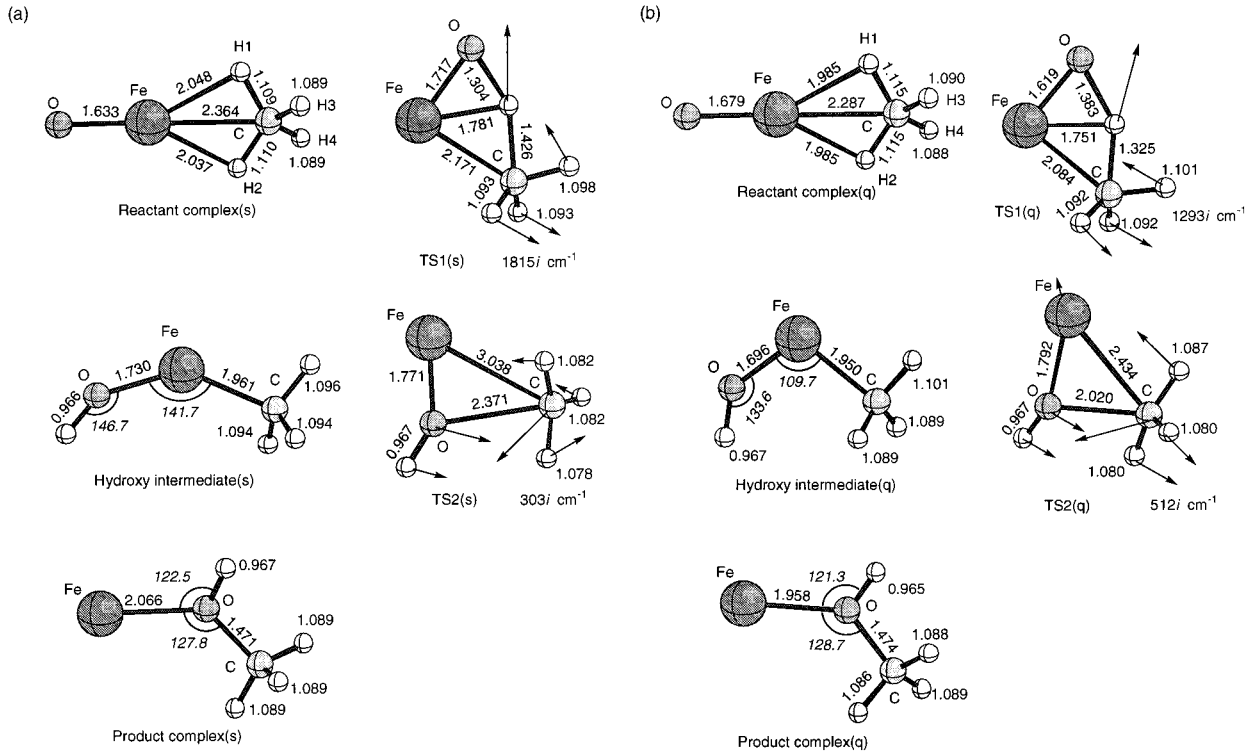

Figure 1. Geometries of the reactant complex, hydroxy intermediate, product complex, and transition states (TSs) along the reaction pathway, $FeO^+ + CH_4 \rightarrow Fe^+ + CH_3OH$, in the (a) sextet and (b) quartet states. Atomic distances in Å and bond angles (italic) in degrees are indicated.

($1\sigma^2 2\sigma^2 1\pi^3 1\delta^2 2\pi^2 3\sigma^1$) and $^3\Delta_1$ ($1\sigma^2 2\sigma^2 1\pi^4 1\delta^3 2\pi^0 3\sigma^1$) states are high-lying in energy as compared with the nearly-degenerate $^5\Sigma^+$ and $^5\Pi$ states.[12h,i] The low-lying low-spin excited states of FeO^+ and CoO^+ are $^4\Delta$ ($1\sigma^2 2\sigma^2 1\pi^4 1\delta^3 2\pi^2 3\sigma^0$) and $^3\Sigma^-$ ($1\sigma^2 2\sigma^2 1\pi^4 1\delta^4 2\pi^2 3\sigma^0$), respectively. These low-spin states have been proposed to be comparable to the reactive $^1\Delta_g$ state of dioxygen and play a significant role in their reactivity with methane,[12h] as we will see later in this paper.

We calculated the electronic structures of these metal-oxide ions within the framework of the B3LYP/6-311G** method to evaluate the binding energies for the reactant complexes. The results are, of course, qualitatively consistent with previous density functional calculations at a different level and higher-level CAS−SCF (complete active space, self-consistent field) calculations.[12d,e,h]

Methane−Methanol Conversion by FeO^+

Each reaction pathway for the methane−methanol conversion by FeO^+ basically includes one intermediate and two TSs as well as reactant and product complexes, as indicated in Scheme 1. We have recalculated all the reactant complexes, intermediates, product complexes, and transition states (TSs) in both the sextet and quartet states at the level of B3LYP/6-311G**. The energetics of the present higher-level calculations is essentially not different from our previous B3LYP/6-311G**//B3LYP/3-21G* calculations.[22] The first reaction pathway, including an important insertion intermediate species, $HO-Fe^+-CH_3$, was confirmed again to be energetically more favorable. The second reaction pathway via a different intermediate, $H-Fe^+-OCH_3$, that is high-lying in energy was less important in the present higher-level calculations. We therefore concentrate here mainly on the reaction pathway via the hydroxy intermediate. The other reaction pathway via the methoxy intermediate will be discussed separately in a future study.

In the course of the entire reaction pathways in Scheme 1, concerted hydrogen and methyl migrations lead to the final product complex. This is an important conclusion from our IRC analyses.[22] Let us look at the reaction pathway via the hydroxy intermediate, $HO-Fe^+-CH_3$. Figure 1 shows the optimized geometries of $OFe^+(CH_4)$, $HO-Fe^+-CH_3$, $Fe^+(CH_3OH)$, and TSs along the preferred reaction pathway in the high-spin sextet and low-spin quartet states, respectively. Important atomic distances and bond angles are indicated in these illustrations. Transition vectors and corresponding imaginary frequencies are shown in the TS structures.

Scheme 3

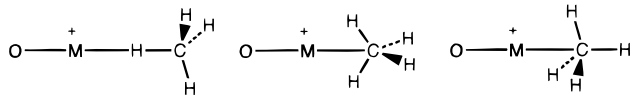

We previously reported these geometries optimized at the B3LYP/3-21G* level[22] so that we do not discuss these in the present paper. The geometries optimized at the 3-21G* and 6-311G** levels are essentially not different. Only in the reactant complex we found a slight difference between the 3-21G* and 6-311G** structures. The structure of the reactant complex optimized with the 6-311G** basis set has an η^2-CH_4 binding mode in contrast to the 3-21G* structure with an η^3-CH_4 binding mode; see Scheme 3. We think that this difference would arise from a set of p-type polarization functions added to hydrogen in the 6-311G** basis set. The coordinated methane is significantly deformed from the T_d-type structure with H−C−H angles of 109.5°. The H1−C−H2 and H3−C−H4 angles of the coordinated methane indicated in Figure 1 were optimized to be approximately 120° and 112°, respectively. The geometry of the methane in the η^2-CH_4 mode belongs approximately to the D_{2d} (more precisely C_{2v}) point group and that in the η^3-CH_4 mode to the C_{3v} point group.[22]

Koga and Morokuma[19a] compared different binding modes of the methane−$RhCl(PH_3)_2$ complex using an ab initio ECP

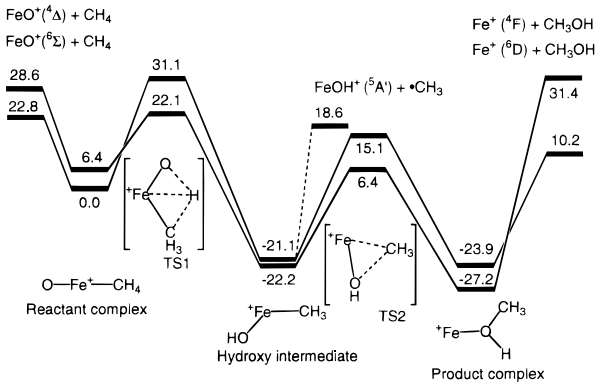

Figure 2. Potential energy diagrams along the reaction pathway, $FeO^+ + CH_4 \rightarrow Fe^+ + CH_3OH$, in the sextet and quartet states. Relative energies are in kcal/mol.

(effective core potential) method and concluded that the η^2-CH_4 mode is energetically most stable and that the end-on mode is unstable. The computed energy difference between the η^2- and η^3-binding modes is rather small (4 kcal/mol), and we think that these structures may coexist very closely on a potential energy surface. However, we do not pursue detailed geometry optimizations for the methane−FeO^+ complex because our main concern is to obtain the important potential energy surfaces along the methane−methanol conversion. The Fe−C bond distances of 2.2−2.3 Å in both spin states are reasonable for these kinds of complexes.

The formation of the Fe−C bond as well as Fe−H bonds in the $OFe^+(CH_4)$ complex is theoretically quite interesting. Both the interaction between the HOMO of the coordinated methane (C−H bonding) and the unfilled orbitals of FeO^+ and the interaction between the LUMO of the methane (C−H antibonding) and the filled orbitals of FeO^+ play an essential role in the formation of this complex.[15] Once this complex is formed, the C−H bonds of the coordinated methane are significantly weakened, due to both orbital interactions, as discussed later in this paper.

One of the hydrogens in the coordinated methane shifts to the ferryl oxygen in a concerted manner via a four-centered transition state, TS1, giving rise to the hydroxy intermediate, $HO-Fe^+-CH_3$. If the reactions, $FeO^+ + CH_4 \rightarrow OFe^+(CH_4) \rightarrow HO-Fe^+-CH_3$, proceed very rapidly, one may think as if a hydrogen atom of the hydrocarbon is directly abstracted by the ferryl "oxygen". However, the real situation is that the hydrogen abstraction follows the formation of the reactant complex, as we saw above. The Fe−O distance in this intermediate is rather short; 1.730 and 1.696 Å in the sextet and quartet states, respectively. Since the total charge of the OH group is almost neutral, these short distances seem very reasonable. Moreover, a methyl migration occurs to form a C−O bond also in a concerted manner via a three-centered transition state, TS2, to lead to the product complex, $Fe^+(CH_3OH)$.

In Figure 2, we show the potential energy diagrams in the sextet and quartet states along the entire reaction pathway, $FeO^+ + CH_4 \rightarrow Fe^+ + CH_3OH$, in which one important reaction intermediate and two TSs as well as reactant and product complexes are included. The potential energy surface of the quartet state is flat as compared with that of the sextet state so that the quartet potential energy surface probably provides a low-energy reaction pathway.[12h]

We find two important crossings between the sextet and quartet potential energy surfaces near the reactant complex and the product complex, as shown in Figure 2. Danovich and Shaik[33] recently carried out detailed spin−orbit coupling calculations along the reaction pathway for the conversion of H_2 to H_2O by FeO^+; $FeO^+ + H_2 \rightarrow OFe^+(H_2) \rightarrow Fe^+(H_2O) \rightarrow Fe^+ + H_2O$. This process also involves two spin-inversion junctions between the sextet and quartet surfaces near the $OFe^+(H_2)$ complex at the entrance channel and near the $Fe^+(H_2O)$ complex at the exit channel. The spin inversion near the reactant complex in the methane−methanol conversion by FeO^+ is quite similar to that in the H_2-H_2O conversion. However, it is a little different in the exit channel for the CH_4-CH_3OH and H_2-H_2O conversions. The crossing between the two surfaces of the FeO^+-CH_4 reaction in the exit channel occurs when $Fe^+(CH_3OH)$ dissociates; in contrast, that of FeO^+-H_2 occurs before the formation of $Fe^+(H_2O)$. Study of spin−orbit coupling in the reaction between FeO^+ and methane seems to be very interesting. Detailed analysis of the seam of crossing between the sextet and quartet potential energy surfaces is also important to understand the spin inversion process for the methane−methanol conversion, as one of the reviewers of this paper suggested. According to the discussion on the dihydrogen activation by FeO^+,[33] the system would not necessarily invert the spin at the lowest energy crossing point under gas-phase conditions.

The binding energies for the reactant complex, $OFe^+(CH_4)$, described above were calculated to be 22.8 and 22.2 kcal/mol in the sextet and quartet states, respectively. The ground state of this complex is a sextet. The most important activation energy from $OFe^+(CH_4)$ to $HO-Fe^+-CH_3$ via TS1 was calculated to be 31.1 kcal/mol on the sextet potential surface; however, it is significantly decreased to 22.1 kcal/mol if a sextet−quartet spin inversion occurs, as shown in Figure 2. Although one would need to estimate a spin−orbit coupling constant for a more detailed understanding, a spin inversion is most likely to occur, while the reaction proceeds from $OFe^+(CH_4)$ to $HO-Fe^+-CH_3$. TS1 is associated with a C−H bond cleavage of methane, but these activation energies, especially the value derived from a spin-inversion process, are rather small as compared with a C−H bond energy of more than 100 kcal/mol.[1−8] These small activation energies will be ascribed later in this paper to C−H bond activation by significant orbital interactions in the reactant complex. The reason we prefer the concerted mechanism for the methane−methanol conversion is based on the computed energetics indicated above.

On the other hand, the activation energy from $OFe^+(CH_4)$ to the methoxy intermediate indicated in Scheme 1, $H-Fe^+-OCH_3$, was computed to be quite large: 61.5 and 39.7 kcal/mol in the sextet and quartet states, respectively. These values are greater than activation energies of 31.1 and 15.7 kcal/mol for the creation of the hydroxy intermediate in the sextet and quartet states, respectively. From the structures of TS1 and TS3 in Scheme 1, we think that the Fe−C bond in TS1 contributes to its greater stability rather than the Fe−H bond in TS3. Thus, the reaction pathway via the methoxy intermediate is energetically less favorable and is unlikely to play a role in the methane−methanol conversion by FeO^+ so that we do not discuss the methoxy intermediate pathway in this paper.

Let us next consider the reaction mechanism how the hydroxy intermediate, $HO-Fe^+-CH_3$, is formed. It is important to note that this intermediate is not created from a direct hydrogen abstraction of methane by the ferryl "oxygen". Before a C−H bond dissociation, the methane in the reactant complex is significantly activated through the formation of an Fe−C bond as well as Fe−H bonds, due to the important orbital interactions

(33) Danovich, D.; Shaik S. *J. Am. Chem. Soc*. **1997**, *119*, 1773.

mentioned above. The methane activation that occurs through the formation of the reactant complex significantly weakens the C−H bonds and facilitates the concerted hydrogen shift with a low activation energy.

The ground state of HO−Fe^+−CH_3 is a low-spin quartet, lying 1.1 kcal/mol below the sextet state, as shown in Figure 2. As we will see later in this paper, the ground state of HO−Co^+−CH_3 is also a low-spin triplet that lies about 5 kcal/mol below a high-spin quintet. These calculational results are consistent with the energetics for a similar intermediate for the H_2−H_2O conversion by FeO^+; the ground state of HO−Fe^+-H was calculated to be a low-spin quartet.[12e]

Since HO−Fe^+−CH_3 is low-lying in energy, the activation energy from HO−Fe^+−CH_3 to $Fe^+(CH_3OH)$ via TS2 that would determine the methanol branching ratio is unfortunately rather high: 36.2 kcal/mol in the sextet state and 28.6 kcal/mol in the quartet state. In contrast to the process from $OFe^+(CH_4)$ toward HO−Fe^+−CH_3, a spin inversion is unlikely to play an essential role here. This activation energy must be small if we expect an efficient methane−methanol conversion. The product branching ratios in FeO^+ shown in Table 1 suggests that there might exist another reaction pathway that leads to the formation of methyl radical: HO−Fe^+−CH_3 → HO−Fe^+ + •CH_3. We also calculated the dissociation energy for this reaction; it is comparable to the activation energy from HO−Fe^+−CH_3 to $Fe^+(CH_3OH)$. We will discuss this dissociation pathway from HO−Fe^+−CH_3 in a later section of this article.

Let us finally look at the process for an elimination of methanol from the product complex. As shown in Figure 2, a spin inversion occurs again during this process. The dissociation energy was calculated to be 58.6 kcal/mol on the sextet potential surface, and it is decreased to 37.4 kcal/mol if we take a crossing between the sextet and quartet surfaces into account. The energy splitting between Fe^+ (^{6}D) and Fe^+ (^{4}F) was calculated to be 11.2 kcal/mol; this is qualitatively consistent with an experimental value of 6.4 kcal/mol.

Methane−Methanol Conversion by MnO^+ and CoO^+

Having described the reactions between FeO^+ and methane, let us next look at the reactivity of MnO^+ (and CoO^+) with methane. We report for the first time ab initio quantum chemical analyses for the methane−methanol conversion by MnO^+ and CoO^+. A comparison of the reactivity in these metal-oxide ions would be quite important for the molecular design of a high-quality catalytic system that converts methane to methanol efficiently. We have confirmed that the reaction between MnO^+ (CoO^+) and methane is essentially similar to the prototype reaction by FeO^+.

Experiments carried out in Schwarz's group[12i] have shown that MnO^+ reacts with methane more efficiently than any other first-row transition-metal-oxide ions, to predominantly afford $MnOH^+$ + •CH_3, with a small fraction of methanol, as listed in Table 1. Thus, if we expect only formation of methanol, MnO^+ is not efficient compared with FeO^+, despite its high reactivity. According to high-level ab initio calculations on the reaction of MnO^+ with dihydrogen,[12h,i] single-state reactivity in MnO^+ would play a dominant role in activating C−H bonds of hydrocarbons in contrast to FeO^+−CuO^+ in which two-state (high-spin and low-spin) reactivity through spin−orbit coupling is very important.

The geometries of the reactant complex, intermediate, product complex, and TSs in the septet and quintet states along the reaction pathway, MnO^+ + CH_4 → Mn^+ + CH_3OH, can be seen in Supporting Information of this paper. The structures

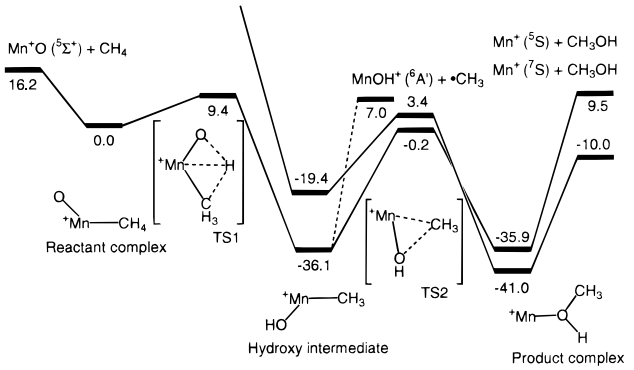

Figure 3. Potential energy diagram along the reaction pathway, MnO^+ + CH_4 → Mn^+ + CH_3OH, in the quintet state. Relative energies are in kcal/mol.

are very similar to those of FeO^+ shown in Figure 1, except for the reactant complex. In $OMn^+(CH_4)$, the binding of methane is of η^3-type in contrast to the binding in $OFe^+(CH_4)$ that displays an η^2-CH_4 binding mode. As suggested by Morokuma and collaborators,[19a−c,f] these two binding modes are close in energy and it depends on spin states which of the two is energetically more favorable. At present it seems to be difficult to say which is preferred in the $OM^+(CH_4)$ complexes of different transition-metal-oxide ions with different spin states. We should mention that in both the structures the methane is significantly deformed from the T_d-type geometry of free methane into a D_{2d} (more precisely C_{2v}) or C_{3v} structure, due to complex formation.

Figure 3 shows the potential energy diagrams along the entire reaction pathway, MnO^+ + CH_4 → Mn^+ + CH_3OH, in the septet and quintet states. The general features of Figure 3 are quite different from those of the potential energy surfaces for the FeO^+ case shown in Figure 2. Since the high-spin septet potential energy surface lies above the low-spin quintet one, a crossing between the septet and quintet surfaces occurs only once near TS2, in contrast to the FeO^+ and CoO^+ cases. This is consistent with the prediction for the reaction between MnO^+ and H_2, as discussed in refs 12h and 12i. Thus, only the quintet state plays an essential role in the first half of the entire reaction, i.e., a C−H bond cleavage step via TS1. The septet state would contribute to the reaction in the final dissociation step in which the product complex dissociates to methanol and the Mn^+ ion.

Very interestingly, the activation energy from $OMn^+(CH_4)$ to HO−Mn^+−CH_3 via TS1 is only 9.4 kcal/mol. This value is much smaller than 31.1 and 22.1 kcal/mol for the FeO^+ cases. As we will see later, this activation energy is also much smaller than those for CoO^+ cases. We therefore think that the activation energy from $OM^+(CH_4)$ to HO-M^+−CH_3 via TS1 would determine the reaction efficiency of metal-oxide ions with methane. Table 1 would suggest that the products shown there are created from the hydroxy intermediate, HO−M^+−CH_3.[12a,b] The low activation energy of 9.4 kcal/mol that we obtained would explain the high reaction efficiency of MnO^+ if we assume that the efficiency of the reaction between the metal-oxide ions and methane is associated with the formation of the hydroxy intermediate, HO−M^+−CH_3. That one can explain the reaction efficiency of MO^+ complexes on the basis of the barrier height of TS1 is one of the most significant points we would like to state in this paper.

The activation energy from HO−Mn^+−CH_3 to $Mn^+(CH_3OH)$ via TS2 was computed to be 35.9 kcal/mol. Interestingly, this value is greater than the 28.6 kcal/mol for the TS2 connecting HO−Fe^+−CH_3 and $Fe^+(CH_3OH)$ in the quartet state,

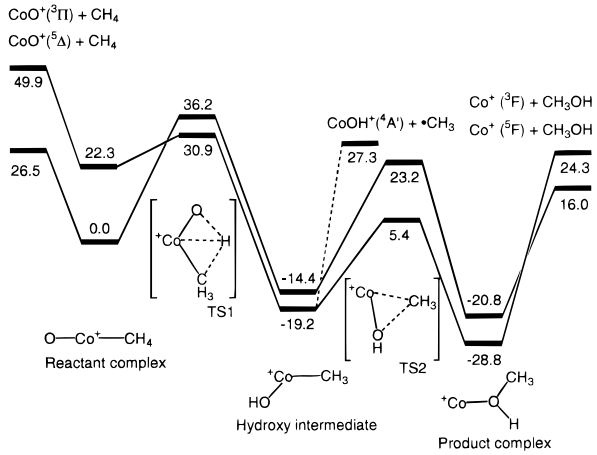

Figure 4. Potential energy diagrams along the reaction pathway, $CoO^+ + CH_4 \rightarrow Co^+ + CH_3OH$, in the quintet and triplet states. Relative energies are in kcal/mol.

whereas the activation energy from $OMn^+(CH_4)$ to $HO-Mn^+-CH_3$ is smaller than that from $OFe^+(CH_4)$ to $HO-Fe^+-CH_3$. We think that these calculational results in MnO^+ and FeO^+ beautifully explain the reason the methanol-branching ratio in MnO^+ (FeO^+) is low (high) despite the high (low) reaction efficiency of MnO^+ (FeO^+). Of course, we should consider the bond dissociation energy for $HO-M^+-CH_3 \rightarrow HO\text{-}M^+ + {}^\bullet CH_3$ along the competitive reaction pathway; we will discuss this later.

Let us finally consider the reactivity of CoO^+ with methane. The mechanisms and energetics in the methane−methanol conversion by CoO^+ have been extensively examined in Armentrout's group.[13j] CoO^+ reacts with methane less efficiently than MnO^+ and FeO^+; however, its methanol branching ratio is interestingly very high. Let us look at how our computations can serve to explain these experimental results. The optimized geometries of $OCo^+(CH_4)$, $HO-Co^+-CH_3$, $Co^+(CH_3OH)$, and TSs along the preferred reaction pathway in the high-spin quintet and low-spin triplet states are shown in Supporting Information. The structures and energetics are quite similar to those of the FeO^+ cases.

Figure 4 shows the potential energy diagrams along the entire reaction pathway, $CoO^+ + CH_4 \rightarrow Co^+ + CH_3OH$, in the quintet and triplet states. The general profiles of the high-spin and low-spin potential surfaces in Figure 4 are quite similar to that of the FeO^+ case. Note that two spin-inversion junctions between the quintet and triplet surfaces are also involved near the $OCo^+(CH_4)$ complex at the entrance channel and near the $Co^+(CH_3OH)$ complex at the exit channel. The important activation energy from $OCo^+(CH_4)$ to $HO-Co^+-CH_3$ is 36.2 kcal/mol on the quintet potential surface, and it decreases to 30.9 kcal/mol if we consider a quintet−triplet spin inversion near TS1. These values appear to be larger than those in FeO^+ as well as in MnO^+. These calculations readily explain an experimental result that the reactivity of CoO^+ is lowest among the three metal-oxide ions in Table 1. In this case, the crossing between the quintet and triplet energy surfaces does not lead to a significant lowering of the activation energy, in contrast to the FeO^+ case.

The second activation energy from $HO-Co^+-CH_3$ to $Co^+(CH_3OH)$ is 37.6 kcal/mol in the quintet state and 24.6 kcal/mol in the triplet state. Although the quintet activation energy is rather large, the triplet one is smaller than 28.6 kcal/mol in the quartet state of FeO^+ and 35.9 kcal/mol in the quintet state of MnO^+. These calculational results thus readily explain the reactivity and catalytic selectivity of CoO^+. Our calculations rationalize the fact that the methanol-branching ratio in CoO^+ is very high, whereas the reaction efficiency of CoO^+ is low. This clearly demonstrates that the low-spin triplet energy surface greatly contributes to the methane−methanol conversion by CoO^+, especially near the reaction pathway between $HO-Co^+-CH_3$ and $Co^+(CH_3OH)$, since the quintet activation energy is high compared with those of FeO^+ and MnO^+. Thus, the spin-inversion processes at the entrance and exit channels play a very significant role in order to afford small potential energy barriers.

The remarkable contrast between the reactivities of MnO^+ and CoO^+ with methane is quite interesting considering the two kinds of activation energies from $OM^+(CH_4)$ to $HO-M^+-CH_3$ and from $HO-M^+-CH_3$ to $M^+(CH_3OH)$. The two activation energies, i.e., the barrier heights of TS1 and TS2, appear to characterize the general features of the methane−methanol conversion by the MO^+ complexes.

Reaction Pathway to Methyl Radical Formation

From Table 1, the formation of methanol competes with that of the methyl radical in the gas-phase reaction between metal-oxide ions and methane, especially in FeO^+. The methyl radical is thus a byproduct for efficient methane−methanol conversion by metal-oxide ions. Therefore we need to consider the energy required for the dissociation reaction, $HO-M^+-CH_3 \rightarrow MOH^+ + {}^\bullet CH_3$, to compare between the two competitive reaction mechanisms.

As already shown in Figures 2−4, we have calculated the lowest dissociation energy for the formation of methyl radical from the hydroxy intermediate in each metal-oxide ion. Let us first look at the dissociation energy for the formation of methyl radical in the CoO^+ cases in which the methyl-radical branching ratio is 0%. As we see in Figure 4, the energy for $CoOH^+$ ($^4A'$) + ${}^\bullet CH_3$ lies 21.9 kcal/mol above TS2 (on the triplet energy surface) that leads to the $Co^+(CH_3OH)$ complex. This dissociation energy is also higher than the dissociation energy from the product complex toward the formation of Co^+ and methanol by approximately 10 kcal/mol. Thus, the methanol-branching pathway is likely to be energetically more preferred from the potential energy profile for the reaction between CoO^+ and methane.

On the other hand, the energy for $MnOH^+$ ($^6A'$) + ${}^\bullet CH_3$ lies only 7.2 kcal/mol above TS2 in the quintet state, as shown in Figure 3. This energy difference in MnO^+ is small compared with 21.9 kcal/mol in CoO^+. Moreover, the dissociation energy for $MnOH^+$ ($^6A'$) + ${}^\bullet CH_3$ is lower than that for the formation of Mn^+ and methanol. On the basis of the relative energy differences, one can conclude that MnO^+ prefers the methyl-radical branching pathway. The remarkable contrast between the calculated potential energy profiles of CoO^+ and MnO^+, shown respectively in Figures 3 and 4, is chemically significant for the prediction of their catalytic selectivity.

We do not repeat a similar discussion for FeO^+. As the reader can see from the potential energy profile in Figure 2, the methanol and methyl-radical branching pathways are competitive in the reaction between FeO^+ and methane.

Methane Activation by Transition-Metal Oxides

We have discussed the preferred reaction pathway for the methane−methanol conversion by MnO^+, FeO^+, and CoO^+; the first step in the proposed mechanism is an encounter in which the MO^+ complex and methane come into contact to form the reactant complex that has an Fe−C bond as well as Fe−H bonds. After the formation of the reactant complex, the

Table 2. Activation Energies from $OM^+(CH_4)$ to $HO-M^+-CH_3$ (ΔE_1) via TS1 and $HO-M^+-CH_3$ to $M^+(CH_3OH)$ (ΔE_2) via TS2 along the Reaction Pathway, $MO^+ + CH_4 \rightarrow M^+ + CH_3OH$[b]

MO^+ (spin state)	ΔE_1 (kcal/mol)	ΔE_2 (kcal/mol)
MnO^+ (quintet)	9.4	35.9
FeO^+ (sextet)	31.1	36.2
FeO^+ (sextet−quartet)	22.1	
FeO^+ (quartet)	15.7[a]	28.6
CoO^+ (quintet)	36.2	37.6
CoO^+ (quintet−triplet)	30.9	
CoO^+ (triplet)	8.6[a]	24.6

[a] Although ΔE_1s on the low-spin potential surfaces of FeO^+ and CoO^+ are small, they do not contribute to the formation of the hydroxy intermediates, due to two-state reactivity, as shown in Figures 2 and 4. [b] For ΔE_1 of FeO^+ and CoO^+, sextet−quartet and quintet−triplet spin inversions are taken into consideration.

Scheme 4

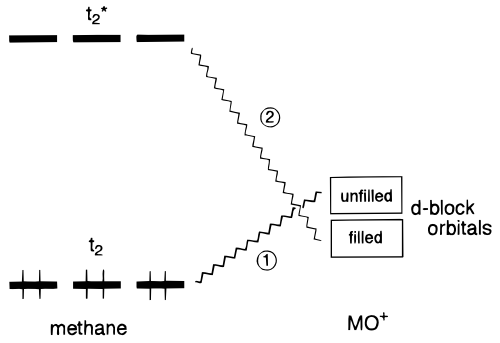

energetics of TS1 and TS2 determines the reactivity and catalytic selectivity for the reaction between MO^+ and methane. We list in Table 2 the two activation energies from $OM^+(CH_4)$ to HO-M^+-CH_3 via TS1 and from $HO-M^+-CH_3$ to $M^+(CH_3OH)$ via TS2. We took a spin inversion effect into account for the former activation energy. The activation energy from the reactant complex to the hydroxy intermediate in MnO^+ was computed to be much smaller than those in FeO^+ and CoO^+. Thus, d^4 oxo complexes would most efficiently activate methane. Let us consider why we can conclude so.

This finding may be rationalized in terms of orbital interactions, following the discussion of Saillard and Hoffmann.[15] As indicated in Scheme 4, both the interaction between the t_2 HOMO of methane (C−H bonding) and the unfilled orbitals of transition-metal-oxide ions, encircled 1, and the interaction between the t_2* LUMO of methane (C−H antibonding) and the filled orbitals of transition-metal-oxide ions, encircled 2, play an essential role in the formation of the reactant complex from which methane activation is most likely to proceed. These 3-fold degenerate HOMO and LUMO may be slightly split, due to deformation of the coordinated methane.

Both the interactions, encircled 1 and 2, significantly weaken the C−H bonds of methane because of the depopulation of C−H bonding orbitals and the occupation of C−H antibonding orbitals, respectively. If the two interactions, encircled 1 and 2, work in approximately equal weight, d^5 complexes may be most effective for the activation of methane. However, since the LUMO of methane is much higher in energy than the d-block orbitals of the MO^+ complexes, the interaction encircled 1 is more dominant than encircled 2 from a qualitative point of view of second-order perturbation theory. Thus, d^4 oxo complexes are rationalized to be most appropriate for methane C−H bond activation in terms of qualitative orbital interaction analyses. In future work we will systematically examine this hypothesis on the basis of high-level ab initio calculations and qualitative orbital interaction analyses.

The above discussion may be useful to understand the enzymatic functions of cytochrome P-450[34] and MMO.[10] The active species of these enzymes, compound I of P-450 and intermediate Q of MMO, involve one or two d^4 Fe(IV)═O (ferryl) moieties. In the catalytic cycle of cytochrome P-450 and MMO, abstraction of an H atom from substrate hydrocarbon that leads to the formation of carbon radical is widely believed to occur in the first step; however, neither intermediates nor transition states have been confirmed in the direct hydrogen abstraction process. Our two-step concerted pathway via TS1 and TS2 is in remarkable contrast to the conventional radical mechanism for hydroxylations by P-450 as well as MMO (so-called oxygen rebound mechanism).[34] Although in our calculations neither important ligand effects nor protein environment has been taken into account, we expect that a similar two-step mechanism should play a role in enzymatic hydroxylations if coordinatively unsaturated ferryl species is created in the active site of the iron-based enzymes.[35]

Summary and Conclusions

We have theoretically studied the conversion of methane to methanol by the transition-metal-oxide ions, $MO^+ + CH_4 \rightarrow M^+ + CH_3OH$, where M is Mn, Fe, and Co. In conclusion, the methane−methanol conversion by the late transition-metal-oxide ions proceeds in such a way

$$MO^+ + CH_4 \rightarrow OM^+(CH_4) \xrightarrow{[TS1]} HO-M^+-CH_3 \xrightarrow{[TS2]} M^+(CH_3OH) \rightarrow M^+ + CH_3OH$$

On the basis of the two activation energies from $OM^+(CH_4)$ to $HO-M^+-CH_3$ via TS1 and from $HO-M^+-CH_3$ to $M^+(CH_3OH)$ via TS2, we have successfully explained the reactivity and selectivity of the reaction between metal-oxide ions and methane, especially for the methanol-branching pathway. We have demonstrated from high-level density functional calculations that the $HO-M^+-CH_3$ intermediate plays the most important role in the reactions between MO^+ and methane. The efficiency of the reaction between MO^+ complexes and methane is likely to be derived from the activation energy from $OM^+(CH_4)$ toward $HO-M^+-CH_3$. A spin inversion between high-spin and low-spin potential energy surfaces greatly contributes for the reaction of FeO^+ and CoO^+ with methane in the process from the $OM^+(CH_4)$ complex to TS1, in contrast to MnO^+. The high (low) reactivity of MnO^+ (CoO^+) is rationalized by the activation energies: 6.4 kcal/mol for MnO^+, 22.1 kcal/mol for FeO^+, and 30.9 kcal/mol for CoO^+. We have also suggested from qualitative orbital interaction analyses that d^4 metal-oxide ions are likely to be most efficient for methane C−H bond activation.

The methanol-branching ratio that is 100% in CoO^+, 41% in FeO^+, and <1% in MnO^+ has also been rationalized from the activation energy from $HO-M^+-CH_3$ to $M^+(CH_3OH)$: 24.6 kcal/mol in the triplet state in CoO^+, 28.6 kcal/mol in the quartet state in FeO^+, and 36.3 kcal/mol in the quintet state in MnO^+. Furthermore, we have calculated the dissociation energy from $HO-M^+-CH_3$ to $MOH^+ + {}^\bullet CH_3$ and compared the two competitive methanol and methyl-radical branching pathways.

Our calculational results completely agree with experimental results on the reaction efficiency and the product branching ratio shown in Table 1. We have clarified that the barrier heights of

(34) *Cytochrome P450: Structure, Mechanism, and Biochemistry*, 2nd ed.; Ortiz de Montellano, P. R., Ed.; Plenum: New York, 1995.
(35) Yoshizawa, K.; Ohta, T.; Yamabe, T.; Hoffmann, R. *J. Am. Chem. Soc.* **1997**, *119*, 12311−12321.

TS1 and TS2, indicated above in the reaction pathway, are most likely to determine the characteristics of the conversion of methane to methanol by MO^+ complexes. On the basis of energetics of the potential energy surfaces shown in Figures 3−5, the reverse reaction, $M^+ + CH_3OH \rightarrow MO^+ + CH_4$, should also occur, we think. Our theoretical analyses may be useful for the development of a high-quality catalyst that converts methane to methanol efficiently.

Acknowledgment. K.Y. is grateful to Prof. Roald Hoffmann and Dr. Norman Goldberg of Cornell University for helpful discussions and comments. We are grateful to a Grant-in-Aid for Scientific Research from the Ministry of Education, Science, and Culture of Japan and to "Research for the Future" Program from the Japan Society for the Promotion of Science (JSPS-RFTF96P00206) for their support of this work. Computations were partially carried out at the Data Processing Center and Supercomputer Laboratory (Institute of Chemical Research) of Kyoto University.

Supporting Information Available: Figures (4 pages). See any current masthead page for ordering and Internet access instructions.

JA971723U